JPET Fast Forward. Published on May 8, 2019 as DOI: 10.1124/jpet.118.255893
This article has not been copyedited and formatted. The final version may differ from this version.

#255893

Title Page

Inhibitory effect of Jing-Fang powder n-butanol extract and its isolated Fraction D on LPS-induced inflammation in RAW264.7 cells

Zhili Rao[1], Haijuan Cao[1], Boyu Shi, Jie Luo, Xiaobo Liu, Nan Zeng

Department of Pharmacology, College of Pharmacy, Chengdu University of TCM, Chengdu city, Sichuan Province, Chengdu 611137, PR China

Downloaded from jpet.aspetjournals.org at ASPET Journals on April 9, 2024

JPET Fast Forward. Published on May 8, 2019 as DOI: 10.1124/jpet.118.255893
This article has not been copyedited and formatted. The final version may differ from this version.

#255893

Running Title Page

Running title： Anti-inflammatory effect and mechanism of Jing-Fang Powder

Corresponding author: Nan Zeng; College of Pharmacy, Chengdu University of TCM, 1166, Wenjiang District, Chengdu City, Sichuan Province, Chengdu 611137, PR China; Phone: +86 028 61800231. Fax: +86 028 61800231. E-mail: 19932015@cdutcm.edu.cn; The authors (ZR and HC) contributed equally to this work

Number of text pages: 34

Tables: 2

Figures: 6

Number of references: 33

The number of words in the abstract: 241

The number of words in introduction: 497

The number of words in the discussion: 1140

Abbreviations: DMEM, Dulbecco's Modified Eagle Medium; IL-1β, Interleukin-1beta; IL-6, Interleukin-6; iNOS, inducible nitric oxide; JFNE, Jing-Fang powder n-butanol extract; LPS, lipopolysaccharide; Nfκb1, nuclear factor of kappa light polypeptide gene enhancer in B cells 1; NF-κB, nuclear factor-kappa B; NO, nitric oxide; PI3K, phosphoinositide 3-kinase; PKB/AKT, protein kinase B; RELA, v- rel Reticuloendotheliosis Viral Oncogene Homolog A; TNF-α, tumor necrosis factor-alpha.

Recommended section: Cellular and Molecular and Inflammation, Immunopharmacology, and Asthma

Downloaded from jpet.aspetjournals.org at ASPET Journals on April 9, 2024

JPET Fast Forward. Published on May 8, 2019 as DOI: 10.1124/jpet.118.255893
This article has not been copyedited and formatted. The final version may differ from this version.

#255893

Abstract

The Jing-Fang powder n-butanol extract (JFNE) has anti-inflammatory properties; however, its active ingredient remains unknown. In addition, the mechanism by which JFNE exerts its anti-inflammatory effects on lipopolysaccharide (LPS) induced inflammation in RAW264.7 cells is yet to be explored. In this study, JFNE was isolated by chromatography to obtain fraction D. We found that pretreatment of LPS-induced RAW264.7 cells with JFNE and fraction D for 3 h significantly reduced the levels of nitric oxide (NO), interleukin-1beta (IL-1β), and tumor necrosis factor-alpha (TNF-α) in the supernatant of cell cultures, and fraction D could also reduce the level of interleukin-6 (IL-6). In addition,JFNE and fraction D significantly reduced the mRNA expression of inducible nitric oxide synthase (iNOS), IL-6, IL-1β, and TNF-α. JFNE and fraction D significantly inhibited the phosphorylation of proteins and mRNA expression levels of phosphoinositide 3-kinase (PI3K) and protein kinase B (PKB/AKT). Moreover, JFNE and fraction D significantly decreased the mRNA expression of iNOS, v-rel reticuloendotheliosis viral oncogene homolog A (RELA), and nuclear factor of kappa light polypeptide gene enhancer in B cells 1 (Nfκb1), while an increase in the mRNA expression of conserved helix-loop-helix ubiquitous kinase (CHUK) was observed. In addition, JFNE and fraction D down-regulated the protein expression of iNOS, nuclear factor-kappa B (NF-κB) (p50), and phosphorylated NF-κB (p65). These results show that JFNE and its isolated fraction D, exert specific anti-inflammation properties in LPS-stimulated RAW264.7 cells that are regulated by inhibition of the PI3K/AKT and NF-κB signaling pathways.

Keywords: Jing-Fang powder, inflammation, RAW264.7, PI3K/AKT, NF-κB

Downloaded from jpet.aspetjournals.org at ASPET Journals on April 9, 2024

JPET Fast Forward. Published on May 8, 2019 as DOI: 10.1124/jpet.118.255893
This article has not been copyedited and formatted. The final version may differ from this version.

1. Introduction

Schizonepeta tenuifolia Briq. and *Saposhnikovia divaricata* (Turcz.) Schischk., are two traditional Chinese medicines. Jing-Fang powder consists of the two herbs (*w/w* = 1:1), and is typically used to treat exterior syndrome caused by exopathy, measles, skin pruritus caused by rubella and eczema, and to prevent and treat allergic inflammatory diseases such as bronchitis and allergic rhinitis (Yu et al., 2013; Zhe et al., 2013; Que et al., 2016). Recent studies show that the essential oils and decoctions prepared from Jing-Fang powder have anti- inflammatory and anti-allergic properties. Jing-Fang powder n-butanol extract (JFNE) has also been shown to be anti-inflammatory (Liu et al., 2007; Yu et al., 2013). Macrophages play an important role in maintaining cellular homeostasis, by enhancing the immune response during infection (Zhu et al., 2015). The M1 macrophage phenotype is induced by LPS and pro-inflammatory Th1 cytokines such as IFN-γ. When macrophages are exposed to LPS, they induce significant phenotypic changes, which are characterized by the production of pro-inflammatory cytokines including IL-1β, IL-6, IL-12, TNF-α, and iNOS (Van Dyken et al., 2013; Johnston et al., 2012). Conversely, the released cytokines are capable of recruiting adaptive immune cells (such as T- lymphocytes) to neutralize phagocytosed pathogens by producing oxygen, nitrogen free radicals, and secreting a series of inflammatory cytokines, which amplify the Th1 immune response to maintain and promote the inflammatory response (Routray et al., 2016; Nathan et al., 2000). The inflammatory mediators secreted by macrophages induce neutrophil migration to the site of injury, enhancing tissue damage (Takemura et al., 2005; Matthay et al., 2012).The PI3K family plays an important role in transducing intracellular cell signals, and in the pathogenesis of inflammation, obesity, tumors, and immune-mediated diseases (John et al., 2015). Akt is a key protein in the AGC kinase family, which is involved in multiple cellular signaling pathways. AKT, a downstream target of PI3K, can be activated by PI3K phosphorylation (Brown and Banerji 2016). After

Downloaded from jpet.aspetjournals.org at ASPET Journals on April 9, 2024

JPET Fast Forward. Published on May 8, 2019 as DOI: 10.1124/jpet.118.255893
This article has not been copyedited and formatted. The final version may differ from this version.

induction of the PI3K/Akt pathway, phosphorylated Akt activates NF-κB by enhancing the phosphorylation and degradation of the NF-κB inhibitory protein I-kappa B kinase (IKKα) (Shi et al., 2016). NF-κB regulates the expression of thousands of important biological genes, which are necessary for multiple cellular functions. Recent studies demonstrated that the NF-κB subunit plays an important role in controlling inflammation (Nguyen et al., 2013). The activation of NF-κB may increase the levels of pro-inflammatory cytokines (such as TNF-α, IL-6, and IL-1β), chemokines, and adhesion molecules to enhance the inflammatory response. The expression of enzymes regulated by NF-κB, such as iNOS and COX-2, which influence the chemotaxis of large numbers of inflammatory cells, such as neutrophils that infiltrate the tissue and aggregate at the site of inflammation (Zhang et al., 2017).

In this study, LPS-induced RAW264.7 cells were used to observe the anti-inflammatory effects of JFNE and its isolated fraction D *in vitro*, and to determine whether the anti-inflammatory effects of JFNE and fraction D are regulated by the activation of PI3K/AKT and NF-κB signaling pathways that control the release of inflammatory cytokines.

Downloaded from jpet.aspetjournals.org at ASPET Journals on April 9, 2024

JPET Fast Forward. Published on May 8, 2019 as DOI: 10.1124/jpet.118.255893
This article has not been copyedited and formatted. The final version may differ from this version.

2. Materials and Methods

2.1 Preparation and separation of JFNE

Schizonepeta tenuifolia and *Saposhnikovia divaricate* (Taiji Pharmacy, Chengdu China Lot: 160901, 160902) were weighed (3000 g), and a 1:1 ratio was used. The decoction with essential oil was collected and concentrated for extraction with petroleum ether, ethyl acetate, and n-butanol sequentially to obtain JFNE. JFNE (100 g) was separated by silica gel column chromatography with a mobile phase composed of ethyl acetate: methanol (3:1) and eluted. The eluate was evaporated under reduced pressure to obtain 17.74 g of fraction D. JFNE and fraction D were dissolved in dimethyl sulfoxide (DMSO), and 0.25% DMSO was used as the vehicle control during drug administration.

2.2 Experimental cell culture

RAW264.7 cells were purchased from the Shanghai Cell Bank of the Chinese Academy of Sciences and cultured in complete Dulbecco's Modified Eagle Medium (DMEM) containing 10% fetal bovine serum in an incubator at 37°C and 5% CO_2.

2.3 Determination of the effect of test drugs on cell viability by MTT assay

RAW264.7 cells (4×10^4 cells/mL) were uniformly seeded in a 96-well cell culture plate and incubated for 12 h, after culturing with each drug for 6 h, 100 μL of MTT (Cell Proliferation and Cytotoxicity Assay Kit, Beyotime, Chengdu, China) solution (100 μL of medium containing 10 μL of MTT) was added to each well, and cultured for 3 h. The supernatant was carefully removed, and 100 μL of DMSO was added. The optical density value (OD value) of each well was detected at 570 nm.

Downloaded from jpet.aspetjournals.org at ASPET Journals on April 9, 2024

JPET Fast Forward. Published on May 8, 2019 as DOI: 10.1124/jpet.118.255893
This article has not been copyedited and formatted. The final version may differ from this version.

2.4 LPS stimulation and detection of NO, IL-6, IL-1β, and TNF-α in culture supernatant

RAW264.7 cells were seeded in 6-well plates at 5×10^5 cells/mL and cultured for 24 h. The cultured cells were divided into 7 groups including: control，LPS (1 μg/mL), LPS + DMSO, LPS + JFNE (0.5 mg/mL, 0.25 mg/mL), and LPS + fraction D (0.5 mg/mL, 0.25 mg/mL). Each group was pretreated with the corresponding concentration of each drug for 3 h, the blank control group and the LPS-treated group contained an equal volume of DMEM, and the DMSO control group contained the same volume of DMEM with 0.25% DMSO. Four technical replicates per group. After 3 h of treatment, the culture solution was aspirated, with the exception of the blank control group in which DMEM was added. DMEM (1.5 mL) containing 1 μg/mL LPS was added to the other wells for 12 h. The cell culture supernatant was collected, and the content of NO was determined using a Total Nitric Oxide Assay Kit (Beyotime, Chengdu, China). The levels of IL-6, IL-1β, and TNF-α in the cell culture supernatant were determined by ELISA (ExCell Biotechnology Co., Ltd., Shanghai, China) according to the manufacturer's instructions.

2.5 Determination of mRNA expression via RT-PCR

Total cellular RNA was extracted from RAW 264.7 cells using the AxyPrep^{TM} Multi-Source Total RNA Miniprep Kit according to the manufacturer's instructions (Axygen, USA) and cDNA was synthesized from total RNA using the FastQuant RT kit (Tiangen, Beijing, China). The amplification reaction was carried out in a 96-well reaction plate (Bio-Rad, Chengdu, China) in a reaction volume of 20 μL. The primer sequences used in this study are as follows: β-actin-F: 5'-ACAGCTGAGAGGGAAATCGTG-3', β-actin-R: 5'-AGAGGTCTTTACGGATGTCAACG-3'; CHUK-F: 5'-TCTACTCCCCAAGGTGGAAG-3', CHUK-R: 5'-GTCAGAGGATGTTCACGGTC-3' ; IL-1β-F: 5'-CAACTGCACTACAGGCTCCG-3', IL-1β-R: 5'- GTGGGTGTGCCGTCTTTCAT-3'; IL-6-F: 5'-AGACAAAGCCAGAGTCCTTCAG-3', IL-6-R: 5'-

Downloaded from jpet.aspetjournals.org at ASPET Journals on April 9, 2024

JPET Fast Forward. Published on May 8, 2019 as DOI: 10.1124/jpet.118.255893
This article has not been copyedited and formatted. The final version may differ from this version.

AGGAGAGCATTGGAAATTGGG-3'; iNOS-F: 5'-ACCATGAGGCTGAAATCCCA-3', iNOS-R: 5'-TCCACAACTCGCTCCAAGAT-3'; NF-κB1-F: 5'-ATGTAGTTGCCACGCACAGA-3', NF-κB1-R: 5'- GGGGACAGCGACACCTTTTA-3'; PI3K-F: 5'-GATGAGGATTTGCCCCACCA-3', PI3K-R: 5'-TTGACTTCGCCGTCTACCAC-3'; AKT-F: 5'-CCGAGGATGCCAAGGAGATCA-3', AKT-R: 5'-GTAGGAGAACTGGGGGAAGTGC-3'; TNF-α-F:5'-ACGGCATGGATCTCAAAGACA-3', TNF-α-R: 5'-GTGAGGAGCACGTAGTCGG- 3'; RELA-F: 5'-TATCTCGCTTTCGGAGGTGC-3', RELA-R: 5'-GCGTGGAGGAAGACACTTGA-3'. The fold change in target genes between the control and treatment groups were normalized with β-actin expression levels. The changes in gene expression were calculated using $2^{-\Delta\Delta Ct}$.

2.6 Analysis of the effects of JFNE and fraction D on NF-κB signaling pathway by SN50

In order to explore the effects of JFNE and fraction D on NF-κB signaling, 40 μM of SN50, an inhibitor of NF-κB signaling, was added 1 hour before treatment with JFNE and fraction D, the NO content in the cell culture supernatant was determined by Griess method and the protein levels of IL-1β and TNF-α were determined by ELISA.

Downloaded from jpet.aspetjournals.org at ASPET Journals on April 9, 2024

JPET Fast Forward. Published on May 8, 2019 as DOI: 10.1124/jpet.118.255893
This article has not been copyedited and formatted. The final version may differ from this version.

2.7 Western blotting

After treatment with JFNE or fraction D for 3 h, and LPS stimulation for 12 h, 180 μL of RIPA lysate buffer (Beyotime, Chengdu, China) containing 1 mM phenylmethylsulfonyl fluoride (PMSF) (Med chem Express, China) was added to each well to extract the total protein in the cells. The total protein concentration of each sample was determined using the BCA kit (Beyotime, Chengdu, China) and all samples were adjusted to the same concentration. The protein samples were mixed with a 5× loading buffer and denatured in at 95℃. The proteins were separated by SDS-PAGE (8% or 12%) and electrophoretically transferred onto polyvinylidene fluoride membranes. The membranes were labeled with PI3 kinase p85 (19H8) rabbit mAb, phospho-Akt (Ser473) (D9E) XP rabbit mAb, Akt (pan) (C67E7) rabbit mAb, β-Actin (13E5) rabbit mAb, NF-κB1 p105/p50(D4P4D) rabbit mAb (1:1000; Cell Signaling Technology; Cat.# 4257, 4060, 4691, 4970, 13586), anti -NF-κB p65 (phospho S536) rabbit pAb, anti-iNOS/NOS2 rabbit pAb, anti -NFκB p65 rabbit pAb, and anti-GAPDH rabbit pAb (1:1000; Servicebio; Cat. GB11142, GB11119, GB11142, GB11002), overnight at 4℃, then incubated with anti-rabbit IgG HRP-linked secondary antibody (1:2000; Cell Signaling Technology; Cat. No. 7074) at 37℃ for 1 h. Antibody detection was performed using a ChemiDoc XRS+ (BioRad, Hercules, CA, USA) image analysis system.

2.8 Analysis of main components of fraction D by liquid chromatography-mass spectrometry (LC-MS)

Liquid chromatography-mass spectrometry (LC-MS) (Thermo Scientific, UltiMate 3000 LC, Orbitrap Elite) was performed using Waters ACQUITY UPLC HSS T3 (2.1 mm × 100 mm 1.8 μm columns), and the chromatographic separation conditions were as follows: column temperature: 40°C; Flow rate: 0.3 mL/min; mobile phase A: water + 0.1% formic acid; mobile phase B: acetonitrile + 0.1% formic acid; injection volume: 4

Downloaded from jpet.aspetjournals.org at ASPET Journals on April 9, 2024

JPET Fast Forward. Published on May 8, 2019 as DOI: 10.1124/jpet.118.255893
This article has not been copyedited and formatted. The final version may differ from this version.

μL; automatic injector temperature: 4°C, and gradient elution procedures are described in Table 1. The mass spectrometry parameters were as follows: ESI+: capillary voltage: 4 kV; sampling cone: 35 kV; source temperature: 100°C; desolvation temperature: 350°C; cone gas flow: 50 L/h; desolvation gas flow: 600 L/h; extraction cone: 4 V ESI-: capillary voltage: 3.5 kV; sampling cone: 50 kV; source temperature: 100°C; desolvation temperature: 350°C; cone gas flow: 50 L/h; desolvation gas flow: 700 L/h; extraction cone: 4 V. Scan time: 0.03 s; inter scan time: 0.02 s; and scan range: 50-1000 m/z. Data analysis was performed using feature extraction and preprocessing with SIEVE software (Thermo, Sichuan, China), normalized, and edited into a two-dimensional data matrix using excel 2010 software, including retention time (RT), compound molecular weight (comp MW), observations (samples) and peak intensity.

2.9 Statistical methods

The data are presented as mean ± SD. SPSS 20.0 software (SPSS Inc., Chicago, IL, USA) was used to determine one-way analysis of variance (ANOVA) with Fisher's protected least significant difference (LSD) post hoc test in order to determine the significance of multiple comparisons. $p < 0.05$ was considered statistically significant.

Downloaded from jpet.aspetjournals.org at ASPET Journals on April 9, 2024

JPET Fast Forward. Published on May 8, 2019 as DOI: 10.1124/jpet.118.255893
This article has not been copyedited and formatted. The final version may differ from this version.

3. Results

3.1 Effect of JFNE and fraction D on RAW264.7 cell viability by MTT assay

Cells were cultivated with 5×10^{-1} mg/mL to 5×10^{-5} mg/mL of JFNE and fraction D for 6 h, none of which had a significant impact on RAW264.7 cell viability (Figure 1). Therefore, LPS-induced RAW264.7 cells were treated with ≤0.5 mg/mL of JFNE and fraction D for 3 h in the subsequent experiments to determine the mechanism in which JFNE and fraction D exert their anti-inflammatory effects on LPS-induced RAW264.7 cells.

3.2 Effect of JFNE and fraction D on secreted and mRNA expression of NO, IL-6, IL-1β, and TNF-α in RAW 264.7 inflammatory cells

As shown in figure 2, RAW264.7 cells incubated with 1 μg/mL of LPS for 12 h significantly increased the levels of NO, IL-6, IL-1β, and TNF-α in the cell culture supernatant, and the mRNA expression of iNOS, IL-6, IL-1β, TNF-α *($p < 0.01$)* relative to control, confirming the use of LPS-induced RAW264.7 cells as an efficient inflammatory model. Compared to untreated controls, RAW264.7 cells pretreated with 0.5 mg/mL and 0.25 mg/mL of JFNE and fraction D for 3 h had significantly reduced levels of the NO,, IL-1β, and TNF-α in the cell culture supernatants and fraction D could also reduce the level of interleukin-6 (IL-6).($p < 0.05$ or $p < 0.01$). In addition, pretreated with 0.5 mg/mL and 0.25 mg/mL of JFNE and fraction D for 3 h had significantly reduced the mRNA expression levels of iNOS, IL-6, IL-1β, and TNF-α in RAW264.7 cells (Figure 3). These results suggest that both JFNE and fraction D have anti-inflammatory effects in LPS-stimulated RAW264.7 cells.

Downloaded from jpet.aspetjournals.org at ASPET Journals on April 9, 2024

JPET Fast Forward. Published on May 8, 2019 as DOI: 10.1124/jpet.118.255893
This article has not been copyedited and formatted. The final version may differ from this version.

3.3 The effect of JFNE and fraction D on PI3K/AKT signaling in LPS-induced RAW264.7 inflammatory cells

Compared with the control group, RAW264.7 cells treated with 1 μg/mL LPS for 12 h significantly increased the levels of phosphorylated PI3K and AKT proteins, suggesting that LPS stimulation can activate the PI3K/AKT signaling pathway. A 0.5 mg/mL concentration of JFNE and fraction D significantly down-regulated the expression levels of phosphorylated PI3K and AKT proteins in inflammatory cells ($p < 0.05$ or $p < 0.01$), suggesting that the anti- inflammatory effects of JFNE and fraction D are regulated by the inhibition of PI3K/AKT signaling pathway activation.

3.4 Exploring the effect of JFNE and fraction D on NF-κB signaling pathway by SN50

SN50 is a specific inhibitor of NF-κB signaling pathway, and our results show that 40 μM of SN50 significantly reduces the levels of NO, IL-1β, and TNF-α in the cell culture supernatant of RAW264.7 cells ($p < 0.01$ *or* $p < 0.05$). This suggests that NF-κB signaling is activated by LPS stimulation after 12 h, and the upregulation of inflammatory factors (such as NO, IL-1β, and TNF-α) are associated with the activation of NF-κB signaling pathway, as the levels of NO, IL-1β, and TNF-α significantly decreased ($p < 0.01$) in the supernatant of the cells treated with JFNE and fraction D in combination with SN50. A more significant anti-inflammatory effect was observed in the cells co-incubated with SN50 and JFNE or fraction D, compared to treatment with SN50 and JFNE or fraction D alone ($p < 0.05$ or $p < 0.01$) (Figure 5).

3.5 Regulatory effect of JFNE and fraction D on NF-κB signaling and iNOS

Downloaded from jpet.aspetjournals.org at ASPET Journals on April 9, 2024

JPET Fast Forward. Published on May 8, 2019 as DOI: 10.1124/jpet.118.255893
This article has not been copyedited and formatted. The final version may differ from this version.

The expression of iNOS, NF-κB (p50), and phosphorylated NF-κB (p65) proteins in LPS-stimulated RAW264.7 cells significantly increased ($p < 0.05$) after LPS stimulation. 0.5 mg/mL of JFNE and fraction D significantly decreased the protein expression levels of iNOS, NF-κB (p50), and phosphorylated NF-κB (p65) in LPS-stimulated RAW264.7 cells ($p < 0.05$). In addition, the mRNA expression of iNOS, RELA, and NF-κB in response to LPS treatment significantly increased ($p < 0.05$), while the mRNA expression of CHUK decreased ($p < 0.05$). 0.5 mg/mL of JFNE and fraction D significantly decreased the expression of iNOS, RELA, CHUK, and NF-κB mRNA expression in RAW264.7 inflammatory cells ($p < 0.05$), while the expression of CHUK increased, relative to control (Figure 6).

3.6 Main chemical components of fraction D

LC-MS analysis of fraction D identified 201 compounds, with high concentrations of betaine and triphenylphosphine oxide. The relative percentages of the top 20 compounds are shown in Table 2.

Downloaded from jpet.aspetjournals.org at ASPET Journals on April 9, 2024

JPET Fast Forward. Published on May 8, 2019 as DOI: 10.1124/jpet.118.255893
This article has not been copyedited and formatted. The final version may differ from this version.

4. Discussion

Previous studies have shown that Jing-Fang power has specific anti-inflammatory properties (Que et al., 2016; Liu et al., 2007; Liu et al., 2013), and that extracts of JFNE retain these anti-inflammatory effects. In this study, JFNE was separated by silica gel column chromatography in order to explore the properties of the active anti-inflammatory compounds in JFNE. Previous *in vivo* experiments in mice demonstrated that the isolated fraction D significantly inhibited inflammation and swelling of the auricle induced by p-xylene, and inhibited the rate of swelling by nearly 71.96%, suggesting that fraction D isolated from JFNE is anti-inflammatory. In this study, the LPS-induced RAW264.7 macrophage inflammatory model was used to explore the mechanism by which JFNE and fraction D exert their anti-inflammatory effects. We found that the specific anti-inflammatory properties of JFNE and fraction D were associated with the inhibition of PI3K/AKT and NF-κB signaling. In addition, fraction D isolated from JFNE was equally as effective as JFNE.

RAW264.7 is a mouse-derived mononuclear macrophage cell-line, and LPS stimulation of RAW264.7 cells can induce classical M1 activation(Zhu et al., 2015; Van Dyken et al., 2013). M1 macrophages are characterized by the production of high concentrations of pro-inflammatory factors including IL-1β, IL-6, IL-12, TNF-α, and inducible nitric oxide synthase (iNOS); and M1 type macrophage mediated iNOS synthesizes NO through the L-arginine pathway, which plays a key role in promoting the inflammatory response (Kröncke et al., 2010). In addition, macrophages are known to recruit adaptive immune cells such as T-lymphocytes to neutralize intracellular pathogens by generating reactive oxygen species and nitrogen free radicals, and secreting a plethora of inflammatory cytokines to promote an inflammatory response (Nathan et al., 2000), as part of the bacterial infection-type inflammatory responses (Holden et al., 2014). Therefore, the LPS-induced RAW264.7 cell inflammatory model is widely used

Downloaded from jpet.aspetjournals.org at ASPET Journals on April 9, 2024

JPET Fast Forward. Published on May 8, 2019 as DOI: 10.1124/jpet.118.255893
This article has not been copyedited and formatted. The final version may differ from this version.

in anti-inflammatory studies *in vitro*. We show that JFNE and fraction D significantly reduces the mRNA expression, and levels of secreted NO, IL-6, IL-1β, and TNF-α in LPS-induced RAW264.7 inflammatory cells. These results suggest that both JFNE and fraction D have anti-inflammatory effects and that the anti-inflammatory effect of fraction D was comparable to that of JFNE.

The PI3K/AKT pathway is a typical intracellular signaling pathway, and studies have shown that PI3K/AKT signaling is involved in the inflammatory response and can be activated by cell membrane receptor binding. This activation produces phosphatidylinositol-3,4,5-triphosphate and further activates downstream signaling proteins, including AKT (Pritchard et al., 2016; Haijian et al., 2017). The serine-threonine kinase (AKT) is a key member of the family of survival after cell injury proteins (Krasilnikov et al., 2000). Activated AKT subsequently dissociates from the membrane and binds to target sites in the cytoplasm and nucleus that plays a key role in numerous biological responses by phosphorylating a range of intracellular proteins. Recent studies have shown that the PI3K/AKT pathway is necessary for the regulation of acute inflammatory responses *in vivo* and *in vitro* by regulating the activation of the NF-κB pathway via nuclear translocation of NF-κB key proteins (such as NF-κB p50 and RELA p65) (Liu et al., 2017; Iyer et al., 2011). In this study, the effects of JFNE and fraction D on the PI3K and AKT total protein and phosphorylation levels in RAW264.7 cells were observed by western blot. LPS- stimulation significantly increased the phosphorylation and mRNA expression levels of PI3K and AKT in RAW264.7 cells, which were reduced in response to both JFNE and fraction D treatment.

In addition, JFNE and fraction D treatment significantly down-regulates the activation of the PI3K/AKT signaling pathway. SN50, a specific inhibitor of NF-κB signaling, was added to RAW264.7 cells 1 h before LPS stimulation to determine whether the NF-κB signaling pathway was involved in the LPS-induced RAW264.7 cell

Downloaded from jpet.aspetjournals.org at ASPET Journals on April 9, 2024

JPET Fast Forward. Published on May 8, 2019 as DOI: 10.1124/jpet.118.255893
This article has not been copyedited and formatted. The final version may differ from this version.

inflammatory response and to observe whether the anti-inflammatory effect of JFNE and fraction D were related to the inhibition of NF-κB signaling pathway. The results showed that 40 μM of SN50 significantly reduced the levels of NO, IL-1β, and TNF-α in cell culture supernatants, suggesting that NF-κB signaling was activated and elevated levels of inflammatory factors (such as NO, IL-1β, and TNF-α) are associated with activation of the NF-κB signaling pathway. Additionally, the results of combined JFNE or fraction D treatment with SN50 show that the anti-inflammatory effect of JFNE and fraction D are related to the inhibition of the NF-κB signaling pathway.

Western blot analysis determined that JFNE and fraction D significantly decreased the protein levels of NF-κB (p50), phosphorylated NF-κB (p65), and iNOS in LPS-stimulated RAW264.7 cells. Moreover, JFNE and fraction D significantly decreased the mRNA expression of iNOS, RELA, and NF-κB, and increased the mRNA expression of CHUK in RAW264.7 inflammatory cells. These results suggested that the anti-inflammatory effect of JFNE and fraction D are associated with inhibition of the NF-κB pathway.

In view of the anti-inflammatory properties of fraction D, LC-MS combined with compound discovery software by mzcloud, chemspider, and Masslist database were used to analyze and identify the molecular components of fraction D. LC-MS analysis found 216 components consisting of high levels of betaine, triphenylphosphine oxide, choline, 1-linoleoyl-sn-glycero-3-phosphocholine, and Dl-Stachydrine in fraction D. A search of related literature for betaine, triphenylphosphine oxide, choline, 1-linoleoyl-sn-glycero-3-phosphocholine, and Dl-Stachydrine, revealed a great number of anti-inflammation studies on betaine and choline; however, very little data on triphenylphosphine oxide, 1-linoleoyl-sn-glycero-3-phosphocholine, and Dl-Stachydrine exist. Betaine has anti-inflammatory and anti-oxidative properties (Hagar et al., 2014; Guangfu et al., 2018). Mechanistically, betaine exerts its anti-oxidative effects by maintaining thiol levels,

Downloaded from jpet.aspetjournals.org at ASPET Journals on April 9, 2024

JPET Fast Forward. Published on May 8, 2019 as DOI: 10.1124/jpet.118.255893
This article has not been copyedited and formatted. The final version may differ from this version.

particularly GSH levels, to inhibit ROS production (Cholewa et al., 2014), primarily by ameliorating sulfur amino acid metabolism (Craig, 2004). In addition, Kharbanda and colleagues found that betaine prevents nitric oxide synthase 2 (NOS2) expression, a process initiated by inflammation (Kharbanda et al., 2012). Furthermore, betaine also inhibits the activity of some upstream signaling molecules that induce the activation of NF-κB (Kim et al., 2014). Betaine reduces endogenous damage-associated molecular pattern (DAMP) generation to inhibit the NF-κB pathway (Zhang et al., 2013). This study showed that betaine exerts an anti-inflammatory effect via inhibition of NF-κB signaling and is an antioxidant, consistent with our findings. Additionally, the anti-inflammatory effects of betaine are related to the inhibition of NLRP3 inflammasome activation, regulation of energy metabolism, and the mitigation of ER stress and apoptosis (Guangfu et al., 2018). Recent studies have determined that choline plays an important role in macrophage phospholipid metabolism and the inflammatory response (Snider et al., 2018), and Pan ZY found that combined choline and aspirin therapy synergistically attenuated an acute inflammatory response (Pan et al., 2014). Besides,William R Parrish found that choline suppressed TNF release from endotoxin-activated human whole blood and macrophages,which characterize the anti-inflammatory efficacy of choline and demonstrate that the modulation of TNF release by choline was associated with significant inhibition of NF-κB activation and requires α7nAChR-mediated signaling(Williamet al., 2008).Their follow-up studies further confirmed the close relationship between α7 nicotinic acetylcholine receptor signaling and inflammatory response(Yang et al., 2019 ; Silvermanet al., 2014). In summary, betaine and choline may be the main components of fraction D responsible for the anti-inflammatory properties observed.

In conclusion, JFNE and fraction D have anti-inflammatory effects in LPS-induced RAW264.7 cells, which may be due to the inhibition of PI3K/AKT signaling and the

Downloaded from jpet.aspetjournals.org at ASPET Journals on April 9, 2024

JPET Fast Forward. Published on May 8, 2019 as DOI: 10.1124/jpet.118.255893
This article has not been copyedited and formatted. The final version may differ from this version.

regulation of NF-κB pathway activation, however, this anti-inflammatory effect requires further verification *in vivo*.

Downloaded from jpet.aspetjournals.org at ASPET Journals on April 9, 2024

JPET Fast Forward. Published on May 8, 2019 as DOI: 10.1124/jpet.118.255893
This article has not been copyedited and formatted. The final version may differ from this version.

Acknowledgments

This work was supported by the National Nature Science Foundation of China (81473399, J1310034-09); Department Pharmacology, Sichuan Provincial Science and Technology, Sichuan Province Youth Science and Technology Innovation Team(2014TD0007).

Downloaded from jpet.aspetjournals.org at ASPET Journals on April 9, 2024

JPET Fast Forward. Published on May 8, 2019 as DOI: 10.1124/jpet.118.255893
This article has not been copyedited and formatted. The final version may differ from this version.

Authorship Contributions

Participated in research design: Rao and Nan.

Conducted experiments: Rao and Cao.

Contributed new reagents or analytic tools: Luo.

Performed data analysis: Cao and Liu.

Wrote or contributed to the writing of the manuscript: Rao and Cao.

Downloaded from jpet.aspetjournals.org at ASPET Journals on April 9, 2024

JPET Fast Forward. Published on May 8, 2019 as DOI: 10.1124/jpet.118.255893
This article has not been copyedited and formatted. The final version may differ from this version.

References

Brown JS and Banerji U (2016) Maximising the potential of Akt inhibitors as anti-cancer treatments. Pharmacol Ther S0163725816302443.

Burke JE and Williams RL (2015) Synergy in activating class I PI3Ks. Trends Biochem Sci 40(2): 88-100.

Changtian Q, Zhe W, Taoqun W, Feng W, Xi X, and Zhi Z (2016) Study on the mechanism of antiallergic effect of ethyl acetate extraction of jingfang powder in allergic animal models. Pharm Clin Chin Materia Medica.

Cholewa JM, Guimarães-Ferreira L, Zanchi NE (2014) Effects of betaine on performance and body composition: a review of recent findings and potential mechanisms. Amino Acids 46(8):1785-1793.

Craig SA (2004) Betaine in human nutrition. Am J Clin Nutr 80(3):539-549.

Guangfu Z, Fang H, Chenlu W, Pan L, Nengzhang L, Jinping D (2018) Betaine in inflammation: mechanistic aspects and applications. Frontiers in Immunology, 9, 1070-.

Hagar H, Medany AE, Salam R, Medany G E, Nayal OA (2014) Betaine supplementation mitigates cisplatin-induced nephrotoxicity by abrogation of oxidative/nitrosative stress and suppression of inflammation and apoptosis in rats. Exp Toxicol Pathol 67(2): 133-141.

Haijian S, Xuexue Z, Weiwei C, and Liying Q (2017) Hypaphorine attenuates lipopolysaccharide-induced endothelial inflammation via regulation of TLR4 and PPAR-γ dependent on PI3K/Akt/mTOR signal pathway. Int J Mol Sci 18(4): 844-.

Holden JA, Attard TJ, Laughton K M, Mansell A, O'Brien-Simpson NM, and Reynold EC (2014) Porphyromonas gingivalis lipopolysaccharide weakly activates M1 and M2

Downloaded from jpet.aspetjournals.org at ASPET Journals on April 9, 2024

JPET Fast Forward. Published on May 8, 2019 as DOI: 10.1124/jpet.118.255893
This article has not been copyedited and formatted. The final version may differ from this version.

polarized mouse macrophages but induces inflammatory cytokines. Infect Immun 82(10): 4190.

Iyer AK, Azad N, Talbot S, Stehlik C, Lu B, Wang L, Rojanasakul Y (2011) Antioxidant c-flip inhibits FAS ligand-induced NF-κB activation in a phosphatidylinositol 3-kinase/Akt-dependent manner. J Immunol 187(6): 3256-66.

Johnston LK, Rims CR, Gill SE, McGuire JK, and Manicone AM (2012) Pulmonary macrophage subpopulations in the induction and resolution of acute lung injury. Am J Respir Cell Mol Biol 47(4): 417-426.

Kharbanda KK, Todero SL, King AL, Osna NA, McVicker BL, Tuma DJ, Wisecarver JL, Bailey SM (2012) Betaine treatment attenuates chronic ethanol-induced hepatic steatosis and alterations to the mitochondrial respiratory chain proteome. Int J Hepatol (2011-11-8), 2011, 2012(16):962183.

Kim DH, Sung B, Chung HY, Kim ND (2014) Modulation of Colitis-associated Colon Tumorigenesis by Baicalein and Betaine. J Cancer Prev 19(3):153-160.

Krasilnikov MA (2000) Phosphatidylinositol-3 kinase dependent pathways: the role in control of cell growth, survival, and malignant transformation. Biochemistry (Moscow) 65(1): 59-67.

Kröncke KD, Fehsel K, Kolbbachofen V (1995) Inducible nitric oxide synthase and its product nitric oxide, a small molecule with complex biological activities. Biol Chem Hoppe Seyler 376(6):327-43.

Liu X, Zeng N, Zhao L (2007) Experimental study on anti-inflammatory and anti-allergic effects of JingFang powder [J]. Pharm Clin Chin Materia Medica 23(5): 158.

Liu Y, Zhe W, Xiping G, Jing Y, Zhiqiang W, and Min H (2013) The protective effect

Downloaded from jpet.aspetjournals.org at ASPET Journals on April 9, 2024

JPET Fast Forward. Published on May 8, 2019 as DOI: 10.1124/jpet.118.255893
This article has not been copyedited and formatted. The final version may differ from this version.

of jingfang powder's effective extract of anti-inflammatory action on lipopolysaccharide-induced acute lung injury in mice. Pharm Clin Chin Materia Medica.

Matthay MA, Ware LB, Zimmerman GA (2012) The acute respiratory distress syndrome. J Clin Investig 122(8): 2731–2740.

Nathan C and Shiloh MU (2000) Reactive oxygen and nitrogen intermediates in the relationship between mammalian hosts and microbial pathogens. PNAS 97(16): 8841-8848.

Nguyen DP, Li J, Yadav SS, and Tewari AK (2014) Recent insights into NF-κB signalling pathways and the link between inflammation and prostate cancer. BJU Int 114(2): 168-176.

Pan ZY and Wang H. (2014) Synergistic interaction between choline and aspirin against acute inflammation induced by carrageenan and lipopolysaccharide. Int Immunopharmacol 20(1): 229-237.

Pritchard RA, Falk L, Larsson M, Leinders M, and Sorkin LS (2016) Different phosphoinositide 3-kinase isoforms mediate carrageenan nociception and inflammation. Pain 157(1): 137-146.

Routray I and Ali S (2016) Boron induces lymphocyte proliferation and modulates the priming effects of lipopolysaccharide on macrophages. PLoS One 11(3): e0150607.

Shi ZM, Han YW, Han XH, Zhang K, Chang YN, Hu ZM, Qi HX, Ting C, Zhen Z, Hong W(2016) Upstream regulators and downstream effectors of NF-κB in Alzheimer's disease. J Neurol Sci 366: 127-134.

Silverman HA, Dancho M, Regnier-Golanov A, Nasim M, Ochani M, Olofsson PS, Ahmed M, Miller EJ, Chavan SS, Golanov E, Metz CN, Tracey KJ, Pavlov VA(2014) Brain region-specific alterations in the gene expression of cytokines, immune cell markers and

Downloaded from jpet.aspetjournals.org at ASPET Journals on April 9, 2024

JPET Fast Forward. Published on May 8, 2019 as DOI: 10.1124/jpet.118.255893
This article has not been copyedited and formatted. The final version may differ from this version.

cholinergic system components during peripheral endotoxin-induced inflammation.Mol Med 20:601-11.

Liu S, Li X, Wu Y, Duan R, Zhang J, Du F, Zhang Q, Li Y, Li N(2017) Effects of vaspin on pancreatic β cell secretion via PI3K/Akt and NF-κB signaling pathways. PLoS One 12(12): e0189722-.

Snider SA, Margison KD, Ghorbani P, LeBlond ND, O'Dwyer C, Nunes JRC, Nguyen T, Xu H, Bennett SAL, Fullerton MD2 (2018) Choline transport links macrophage phospholipid metabolism and inflammation. J Biol Chem jbc.RA118.003180-.

Takemura Y, Iwasaki Y, Nagata K, Yokomur I, Tando S, and Fushiki S (2005) Influence of depletion of alveolar macrophages on apoptosis in candida-induced acute lung injury. Exp Lung Res 31(3): 307-321.

Van Dyken SJ and Locksley RM (2013) Interleukin-4- and interleukin-13-mediated alternatively activated macrophages: roles in homeostasis and disease. Annu Rev Immunol 31(1): 317-343.

William R Parrish, Mauricio Rosas-Ballina, Margot Gallowitsch-Puerta, Mahendar Ochani, Kanta Ochani, Li-Hong Yang, LaQueta Hudson, Xinchun Lin, Nirav Patel, Sarah M Johnson, Sangeeta Chavan, Richard S Goldstein,Christopher J Czura, Edmund J Miller, Yousef Al-Abed, Kevin J Tracey, and Valentin A Pavlov(2008)Modulation of TNF Release by Choline Requires α 7 Subunit Nicotinic Acetylcholine Receptor-Mediated Signaling.Mol Med 14(9-10): 567-574.

Yang H, Liu H, Zeng Q, Imperato GH, Addorisio ME, Li J, He M, Cheng KF, Al-Abed Y, Harris HE, Chavan SS, Andersson U, Tracey KJ (2019) Inhibition of HMGB1/RAGE-mediated endocytosis by HMGB1 antagonist box A, anti-HMGB1 antibodies, and cholinergic agonists suppresses inflammation.Mol Med25(1):13.

Downloaded from jpet.aspetjournals.org at ASPET Journals on April 9, 2024

JPET Fast Forward. Published on May 8, 2019 as DOI: 10.1124/jpet.118.255893
This article has not been copyedited and formatted. The final version may differ from this version.

Yu L, Wang Z, Xiong R, Gong X, Gou L, Tang Q, Shen C, Zeng N.(2013) Experimental study on the primary screening of effective parts of Jing Fang San with anti-inflammatory and anti-allergic effects . Lishizhen Med Mater Med Res 24(2): 271-273

Zhang H, Shan Y, Wu Y, Xu C, Yu X, and Zhao J et al. (2017) Berberine suppresses LPS-induced inflammation through modulating sirt1/NF-κB signaling pathway in RAW264.7 cells. Int Immunopharmacol 52: 93-100.

Zhe W, Liu Y, Xiping G, Jing Y, Min H, and Zhiqiang W et al. (2013) The anti-allergic effects of ethyl acetate extract of jingfang powder. Pharm Clin Chin Materia Medica 29(5): 92-95.

Zhu L, Zhao Q, Yang T, Ding W, and Zhao Y (2015) Cellular metabolism and macrophage functional polarization. Int Rev Immunol 34(1): 19.

Downloaded from jpet.aspetjournals.org at ASPET Journals on April 9, 2024

JPET Fast Forward. Published on May 8, 2019 as DOI: 10.1124/jpet.118.255893
This article has not been copyedited and formatted. The final version may differ from this version.

Footnotes

Footnote to title:

This work was supported by the National Nature Science Foundation of China [81473399, J1310034-09] and Department Pharmacology, Sichuan Provincial Science and Technology, Sichuan Province Youth Science and Technology Innovation Team[2014TD0007].

Footnotes to authors:

[1] These authors contributed equally to the work.

Downloaded from jpet.aspetjournals.org at ASPET Journals on April 9, 2024

JPET Fast Forward. Published on May 8, 2019 as DOI: 10.1124/jpet.118.255893
This article has not been copyedited and formatted. The final version may differ from this version.

Legends for Figures

Figure 1 The effect of JFNE and fraction D on RAW264.7 cell viability. Cells were cultivated with 5×10^{-1} mg/mL to 5×10^{-5} mg/mL of JFNE and fraction D for 6 h, then 100 μL of MTT was added to observe the effect of each drug on cell viability by measuring the OD value at 490 nm. Data are presented as the mean ± SEM; n = 6.

Figure 2 Effect of JFNE and fraction D on NO, IL-6, IL-1β, and TNF-α in supernatant of LPS-induced RAW264.7 cells. RAW264.7 cells were stimulated with 1 μg/mL LPS for 12 h (LPS), pretreated with fraction D (fraction D + LPS), JFNE (JFNE + LPS), and the same volume of DMEM with 0.25% DMSO (DMSO) for 3 h before LPS was added, the blank control group contained an equal volume of DMEM (Control), the cell culture supernatant was collected and the protein levels of NO, IL-6, IL-1β, and TNF-α were assayed. Data are presented as the mean ± SEM, compared to LPS-only control cells, $*p < 0.05$, $**p < 0.01$; n = 6.

Figure 3 Effect of JFNE and fraction D on mRNA expression of iNOS, IL-6, IL-1β, and TNF-α in LPS-induced RAW264.7 cells. RAW264.7 cells were stimulated with 1 μg/mL LPS for 12 h (LPS), pretreated with fraction D (fraction D + LPS), JFNE (JFNE + LPS), and the same volume of DMEM with 0.25% DMSO (DMSO) for 3 h before LPS was added, the blank control group contained an equal volume of DMEM (Control),the fold change in gene expression was normalized to β-actin expression. The changes in gene expression were calculated using $2^{-\Delta\Delta Ct}$. Data are presented as the mean ± SEM, compared to LPS-only control cells, $*p < 0.05$, $**p < 0.01$ (n = 4).

Figure 4 The effect of JFNE and fraction D on the phosphorylation and mRNA expression levels of PI3K and AKT. (A) After RAW264.7 cells were pretreated with fraction D (fraction D + LPS) or JFNE (JFNE + LPS) and stimulated with 1 μg/mL LPS for 12 h (LPS), the phosphorylation and total protein levels of PI3K and AKT were

Downloaded from jpet.aspetjournals.org at ASPET Journals on April 9, 2024

JPET Fast Forward. Published on May 8, 2019 as DOI: 10.1124/jpet.118.255893
This article has not been copyedited and formatted. The final version may differ from this version.

assayed by western blot. (B) Phosphorylation of PI3K was calculated as the ratio of phosphorylated PI3K (p-PI3K) to total PI3K. (C) The mRNA expression of PI3K was measured by RT-PCR. (D) Phosphorylation of AKT was calculated as the ratio of phosphorylated AKT (p-PI3K) to total AKT. (E) The mRNA expression of AKT was measured by RT-PCR. Data are presented as the mean ± SEM, compared to LPS-only control cells, $*p < 0.05$, $**p < 0.01$ (n = 4).

Figure 5 The effect of JFNE and fraction D treatment combined with NF-κB pathway specific inhibitor SN50 on the expression of NO, IL-1β, and TNF-α in the supernatant of RAW264.7 cells cultures induced by LPS. SN50 (40 μM), an inhibitor of NF-κB signaling, was added 1 h before treatment with JFNE and fraction D, the cell culture supernatant was collected, and levels of NO, IL-1β, and TNF-α were assayed. Compared with the LPS group, $*p < 0.05$, $**p < 0.01$. Compared to JFNE and fraction D treatment alone, $^{\#}p < 0.05$, $^{\#\#}p < 0.01$. Compared to treatment with SN50 alone, $^{\&}p < 0.05$, and $^{\&\&}p < 0.01$.

Figure 6 Effect of JFNE and fraction D on protein levels of p-p65, p65, p50, p105, iNOS and mRNA expression of CHUK and, RELA, and NF-κB in LPS-induced RAW264.7 inflammatory cells. (A) After RAW264.7 cells were pretreated with fraction D (fraction D + LPS) , JFNE (JFNE + LPS) and stimulated with 1 μg/mL LPS for 12 h (LPS), the phosphorylation and protein levels of iNOS, NF-κB p65 (p65), phosphorylated NF-κB p65 (p-p65), NF-κB p50(p50), NF-κB p105 (p105) were assayed by western blotting. (B) The phosphorylation of p65 was calculated as the ratio of p-p65 to GAPDH. (C) The level of p50 was calculated as the ratio of p60 to GAPDH. (D) The protein level of iNOS was calculated as the ratio of iNOS to GAPDH. The mRNA expression levels of (E) CHUK, (F) RELA, and (G) NF-κB were measured by RT-PCR. Data are presented as the mean ± SEM, compared to LPS-only control cells, $*p < 0.05$, $**p < 0.01$ (n = 4).

Downloaded from jpet.aspetjournals.org at ASPET Journals on April 9, 2024

JPET Fast Forward. Published on May 8, 2019 as DOI: 10.1124/jpet.118.255893
This article has not been copyedited and formatted. The final version may differ from this version.

Tables

Table 1 Gradient of mobile phase

Time (min)	Flow rate (mL/min)	A (%)	B (%)
0	0.3	95	5
1	0.3	95	5
2	0.3	60	40
7	0.3	20	80
11	0.3	5	95
15.5	0.3	95	5
19.5	0.3	95	5

Downloaded from jpet.aspetjournals.org at ASPET Journals on April 9, 2024

JPET Fast Forward. Published on May 8, 2019 as DOI: 10.1124/jpet.118.255893
This article has not been copyedited and formatted. The final version may differ from this version.

Table 2 Main chemical components of fraction D by LC-MS

NO.	Name	Molecular	Formula	RT (min)	Percentage (%)
1	Betaine	117.08	$C_5H_{11}NO_2$	1.38	12.57
2	Triphenylphosphine oxide	278.08	$C_{18}H_{15}OP$	5.82	5.63
3	Choline	103.10	$C_5H_{13}NO$	1.34	4.86
4	1-Linoleoyl-sn-glycero-3-phosphocholine	519.33	$C_{26}H_{50}NO_7P$	6.92	4.73
5	DL-Stachydrine	143.09	$C_7H_{13}NO_2$	1.42	3.64
6	O-glutaroyl-L-carnitine	275.14	$C_{12}H_{21}NO_6$	1.42	2.95
7	O-ureido-l-serine	163.06	$C_4H_9N_3O_4$	1.14	2.39
8	(2S)-4-Methyl-2-({[(3S,4S,5R)-2,3,4-trihydroxy-5-(hydroxymethyl)tetrahydro-2-furanyl]methyl}amino)pentanoic acid (non-preferred name)	293.15	$C_{12}H_{23}NO_7$	2.08	2.35
9	Dibutyl phthalate	278.15	$C_{16}H_{22}O_4$	8.14	2.35
10	O-3-methylglutarylcarnitine	289.15	$C_{13}H_{23}NO_6$	1.49	1.78
11	Adenosine	267.10	$C_{10}H_{13}N_5O_4$	2.04	1.71
12	1-oleoylglycerone 3-phosphate	434.24	$C_{21}H_{39}O_7P$	9.05	1.37
13	1-Hexadecanoyl-sn-glycero-3-phosphocholine	495.33	$C_{24}H_{50}NO_7P$	7.32	1.36
14	Leonurine	311.15	$C_{14}H_{21}N_3O_5$	4.34	1.23
15	Adenine	135.05	$C_5H_5N_5$	1.48	1.11
16	Stearamide	283.29	$C_{18}H_{37}NO$	11.32	1.06
17	oleoyl-lysophosphatidylcholine	521.35	$C_{26}H_{52}NO_7P$	7.61	1.01
18	1-Aminocyclohexanecarboxylic acid	143.09	$C_7H_{13}NO_2$	2.06	0.98
19	4-Undecylbenzenesulfonic acid	312.18	$C_{17}H_{28}O_3S$	10.66	0.89
20	1-Palmitoyl lysophosphatidic acid	410.24	$C_{19}H_{39}O_7P$	10.52	0.75

Downloaded from jpet.aspetjournals.org at ASPET Journals on April 9, 2024

JPET Fast Forward. Published on May 8, 2019 as DOI: 10.1124/jpet.118.255893
This article has not been copyedited and formatted. The final version may differ from this version.

Figures

Figure 1

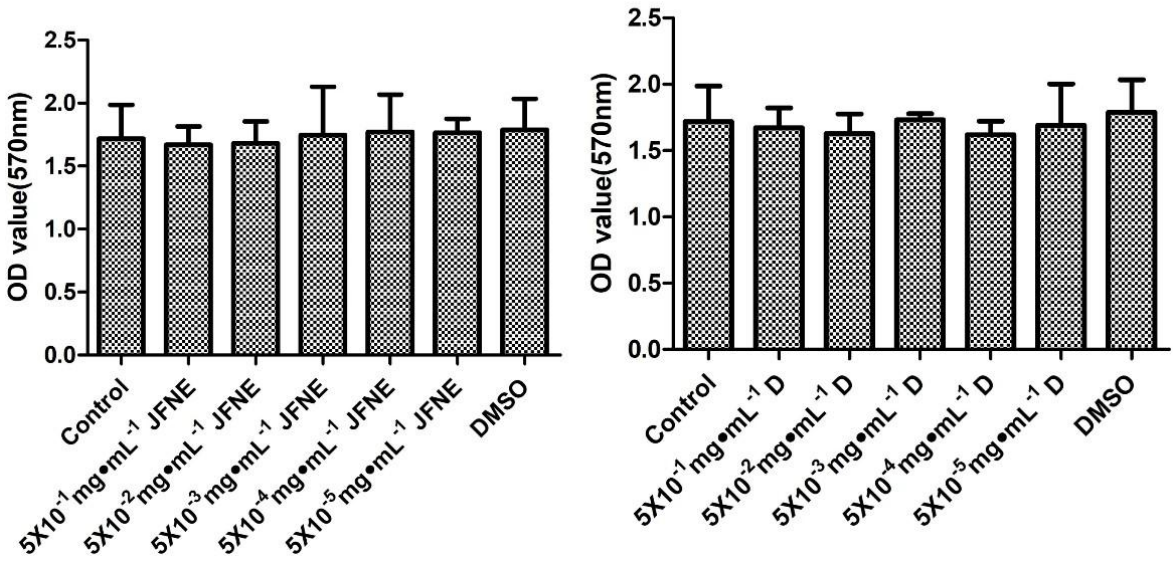

Downloaded from jpet.aspetjournals.org at ASPET Journals on April 9, 2024

Figure 2

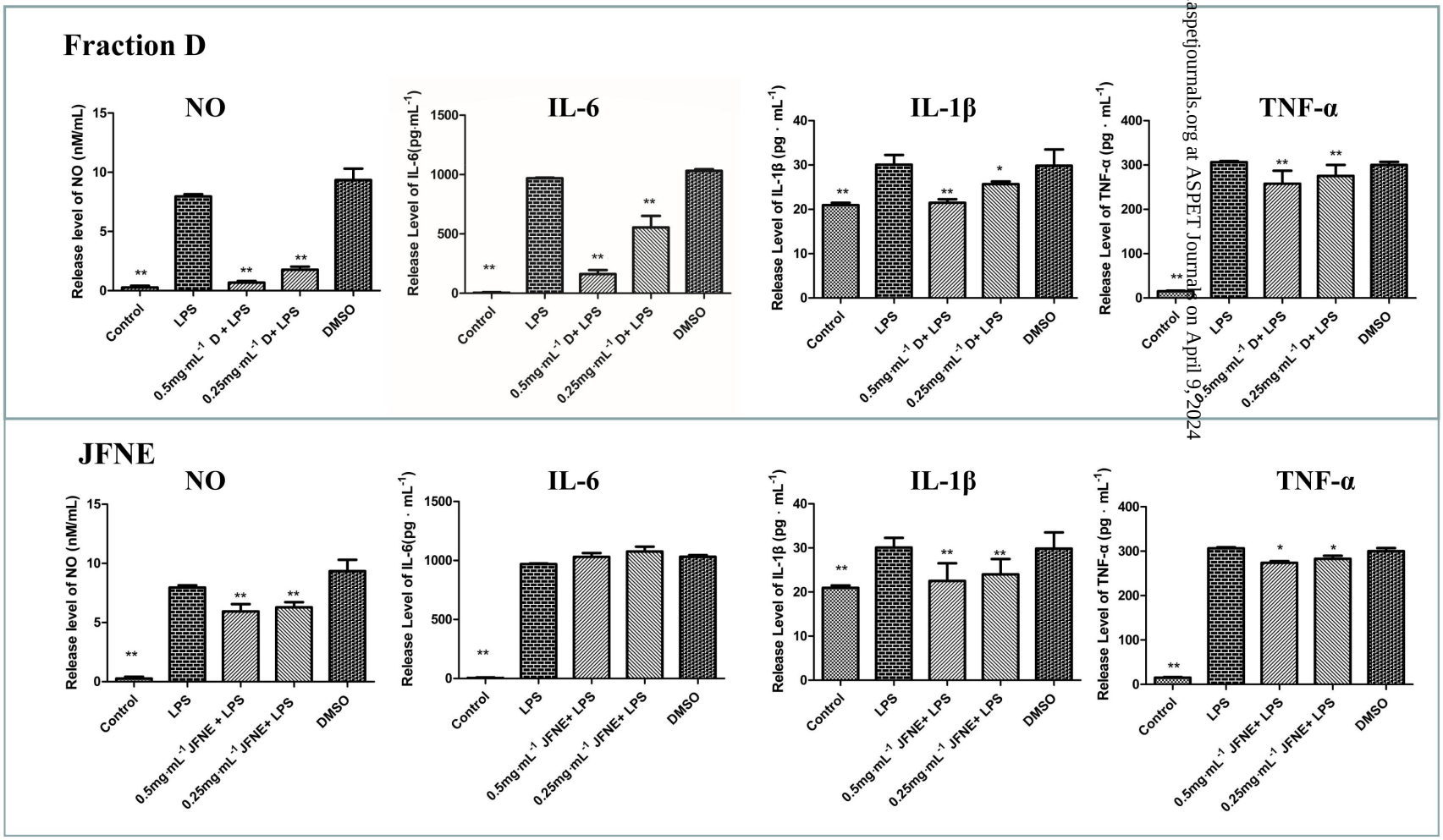

Downloaded from jpet.aspetjournals.org at ASPET Journals on April 9, 2024

JPET Fast Forward. Published on May 8, 2019 as DOI: 10.1124/jpet.118.255893
This article has not been copyedited and formatted. The final version may differ from this version.

Figure 3

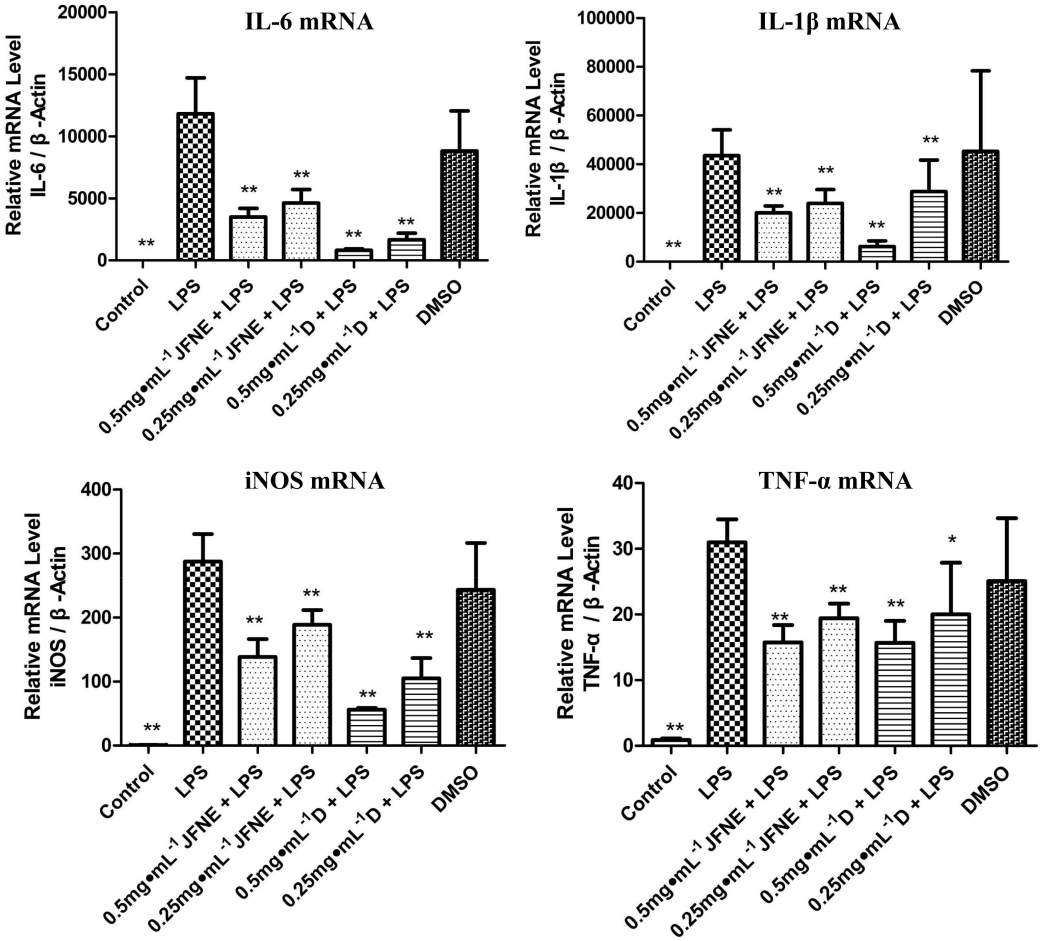

Downloaded from jpet.aspetjournals.org at ASPET Journals on April 9, 2024

JPET Fast Forward. Published on May 8, 2019 as DOI: 10.1124/jpet.118.255893
This article has not been copyedited and formatted. The final version may differ from this version.

Figure 4

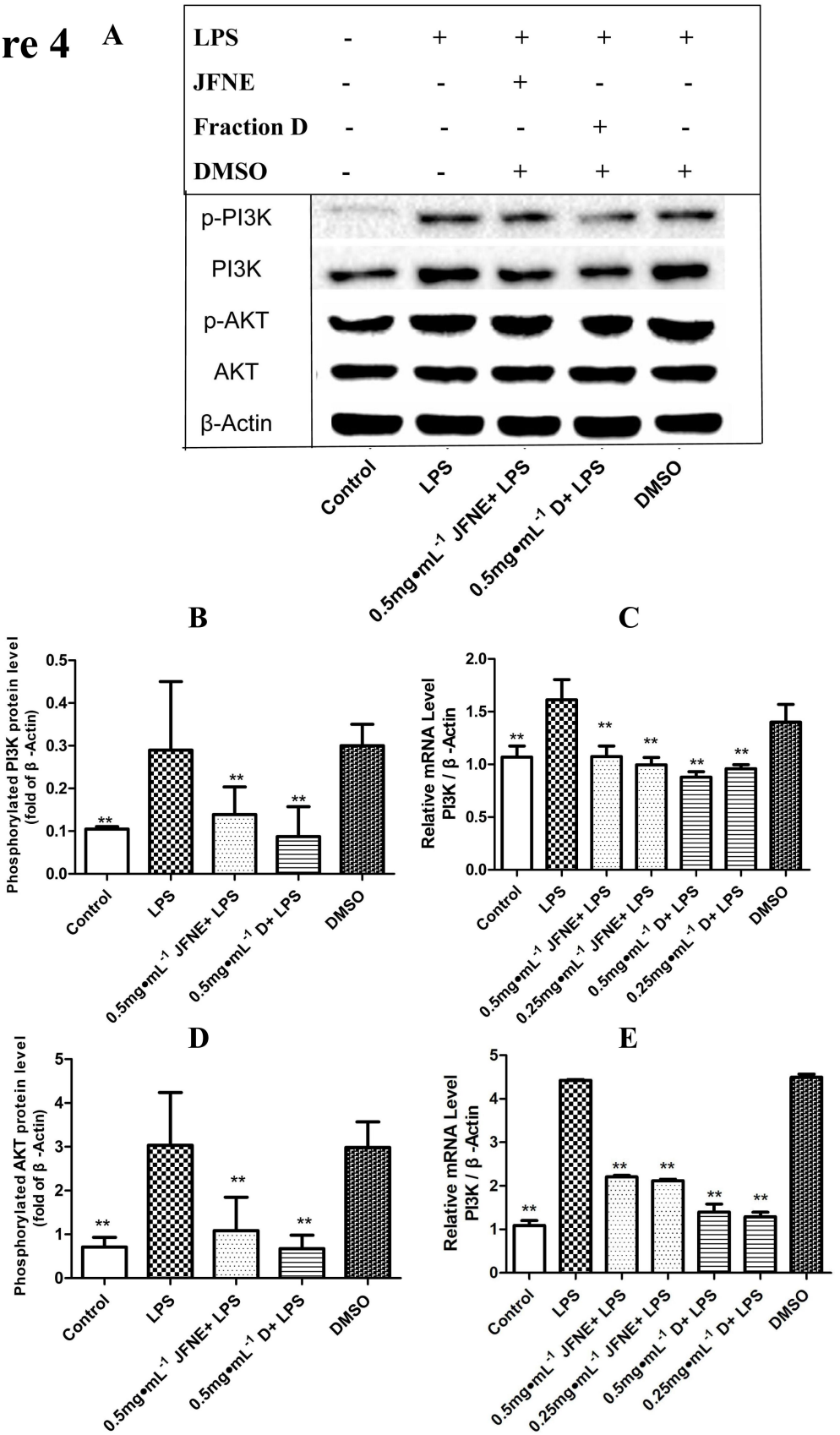

Downloaded from jpet.aspetjournals.org at ASPET Journals on April 9, 2024

JPET Fast Forward. Published on May 8, 2019 as DOI: 10.1124/jpet.118.255893
This article has not been copyedited and formatted. The final version may differ from this version.

Figure 5

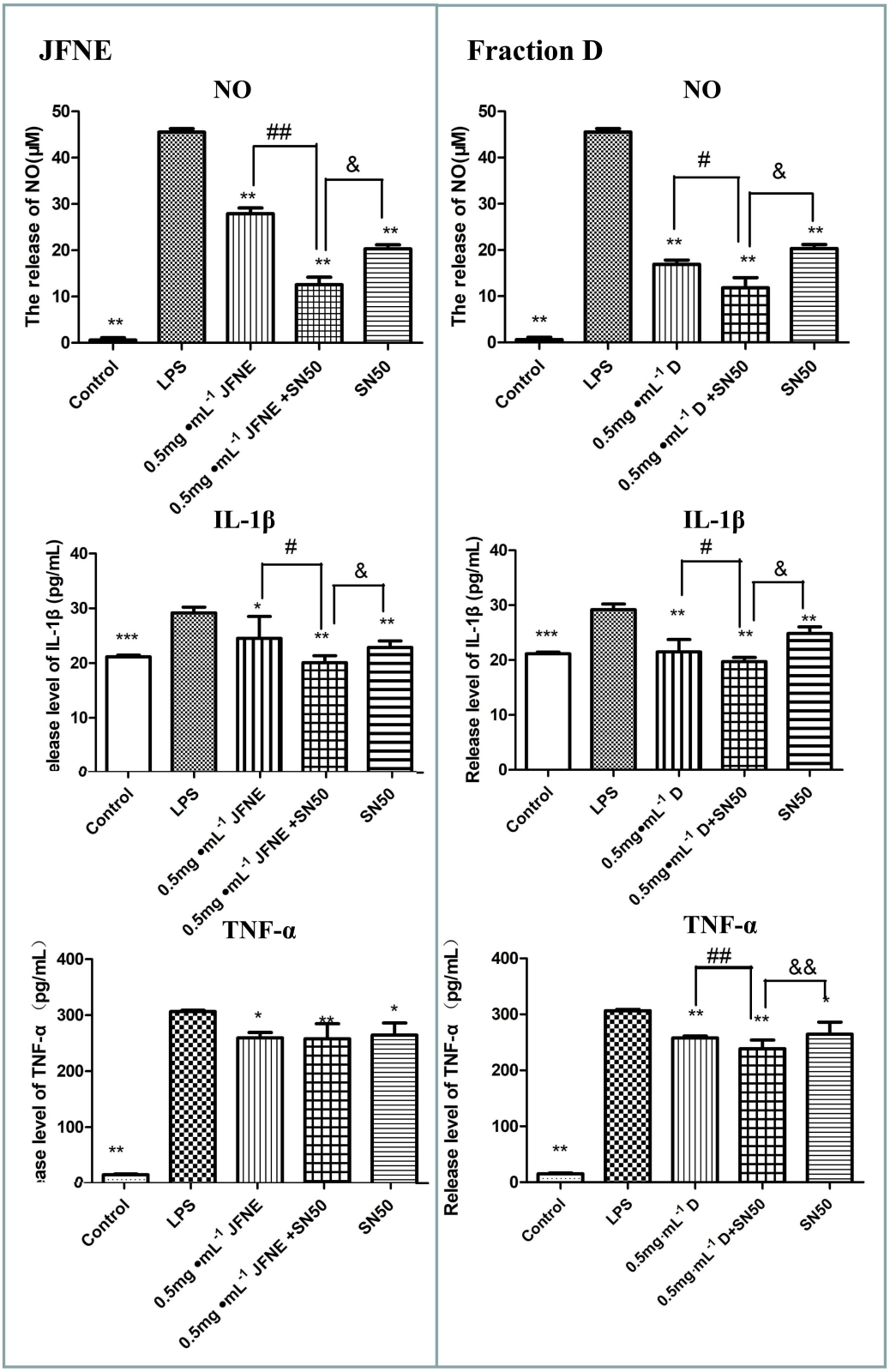

Downloaded from jpet.aspetjournals.org at ASPET Journals on April 9, 2024

JPET Fast Forward. Published on May 8, 2019 as DOI: 10.1124/jpet.118.255893
This article has not been copyedited and formatted. The final version may differ from this version.

Figure 6

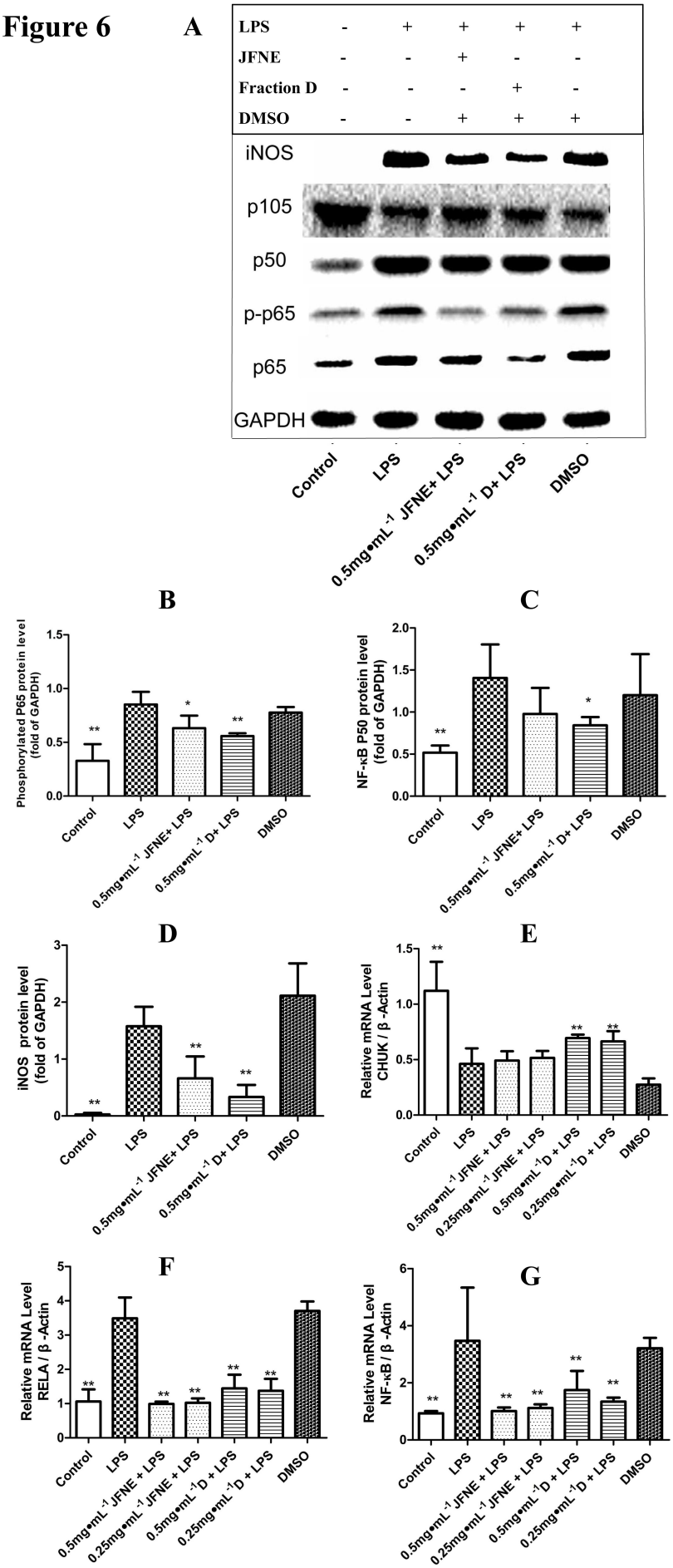

Downloaded from jpet.aspetjournals.org at ASPET Journals on April 9, 2024